J|A|C|S ARTICLES

Published on Web 06/17/2009

Advanced Monte Carlo Approach To Study Evolution of Quartz Surface during the Dissolution Process

Shikha Nangia and Barbara J. Garrison*

104 Chemistry Building, Department of Chemistry, The Pennsylvania State University, University Park, Pennsylvania 16802

Received February 19, 2009; E-mail: bjg@psu.edu

Abstract: A newly developed Monte Carlo (MC) algorithm designed to study the complex interplay of dissolution and precipitation reactions on mineral surface is presented. This algorithm utilizes existing advanced reactive and configurational-biased MC techniques with new protocols specific for mineral−water interfaces. This time-independent methodology is especially advantageous for studying the kinetically slow quartz−water dissolution process. The aim is to use this method to understand the role of the local arrangement of reactive sites and surface topography in the surface evolution during dissolution. The simulations were performed in neutral pH medium, and two possible dissolution mechanisms were tested. The results indicate that out of the direct and stepwise mechanisms, the direct mechanism leads to complete dissolution that is not experimentally observed in the natural environment. On the other hand, the stepwise dissolution is more realistic, as it resembles the experimentally observed steady-state dissolution of the quartz−water system. These simulations identify the least coordinated surface sites (Q^1) as the primary reactive site for hydrolysis and precipitation. Other surface sites (Q^2 and Q^3) also undergo hydrolysis, but they are sterically hindered and are turned passive by precipitating Q^1 groups. The conclusions from the simulations are dominated by the surface topology of quartz; thus, we believe that the results are applicable for other polymorphs of silica and other protonation conditions.

I. Introduction

Quartz (SiO_2) is an abundant mineral in the earth's crust and interacts constantly with water, which covers 71% of the earth's surface. It is therefore very important to understand the chemistry at the quartz−water interface, a topic that has been investigated for decades.[1−32] These investigations can be broadly classified into experimental[1−7,9,10,12−16,19−22,30] and computational studies,[8,11,17,18,23−29,31,32] both of which have evolved considerably over the years. The experimental techniques have evolved from solution chemistry[1,19] in the early investigations to the present direct imaging technologies and surface probes.[33−36] Similarly, with advances in computational power and software, the calculations are no longer limited to isolated small clusters;[8,17,18] rather, inclusion of solvation effects and long-range systems mimicking the bulk mineral is now affordable.[37,38]

(1) Rimstidt, J. D.; Barnes, H. L. *Geochim. Cosmochim. Acta* **1980**, *44*, 1683.
(2) Petrovich, R. *Geochim. Cosmochim. Acta* **1981**, *45*, 1665.
(3) Knauss, K. G.; Wolery, T. J. *Geochim. Cosmochim. Acta* **1987**, *52*, 43.
(4) Schwartzentruber, J.; Furst, W.; Renon, H. *Geochim. Cosmochim. Acta* **1987**, *51*, 1867.
(5) Bennett, P. C.; Melcer, M. E.; Siegel, D. I.; Hassett, J. P. *Geochim. Cosmochim. Acta* **1988**, *52*, 1521.
(6) Brady, P. V.; Walther, J. V. *Chem. Geol.* **1990**, *82*, 253.
(7) Dove, P. M.; Crerar, D. A. *Geochim. Cosmochim. Acta* **1990**, *54*, 955.
(8) Lasaga, A. C.; Gibbs, G. V. *Am. J. Sci.* **1990**, *290*, 263.
(9) Bennett, P. C. *Geochim. Cosmochim. Acta* **1991**, *55*, 1781.
(10) Dove, P. M.; Elston, S. F. *Geochim. Cosmochim. Acta* **1992**, *56*, 4147.
(11) Gratz, A. J.; Bird, P. *Geochim. Cosmochim. Acta* **1993**, *57*, 977.
(12) Gratz, A. J.; Bird, P. *Geochim. Cosmochim. Acta* **1993**, *57*, 965.
(13) Anbeek, C.; Vanbreemen, N.; Meijer, E. L.; Vanderplas, L. *Geochim. Cosmochim. Acta* **1994**, *58*, 4601.
(14) Berger, G.; Cadore, E.; Schott, J.; Dove, P. M. *Geochim. Cosmochim. Acta* **1994**, *58*, 541.
(15) Dove, P. M. *Am. J. Sci.* **1994**, *294*, 665.
(16) Tester, J. W.; Worley, W. G.; Robinson, B. A.; Grigsby, C. O.; Feerer, J. L. *Geochim. Cosmochim. Acta* **1994**, *58*, 2407.
(17) Xiao, Y.; Lasaga, A. C. *Geochim. Cosmochim. Acta* **1994**, *58*, 5379.
(18) Xiao, Y.; Lasaga, A. C. *Geochim. Cosmochim. Acta* **1996**, *60*, 2283.
(19) Rimstidt, J. D. *Geochim. Cosmochim. Acta* **1997**, *61*, 2553.
(20) Johnson, J. W.; Knauss, K. G.; Glassley, W. E.; DeLoach, L. D.; Tompson, A. F. B. *J. Hydrol.* **1998**, *209*, 81.
(21) Dove, P. M. *Geochim. Cosmochim. Acta* **1999**, *63*, 3715.
(22) Schulz, M. S.; White, A. F. *Geochim. Cosmochim. Acta* **1999**, *63*, 337.
(23) Pelmenschikov, A.; Strandh, H.; Pettersson, L. G. M.; Leszczynski, J. *J. Phys. Chem. B* **2000**, *104*, 5779.
(24) Pelmenschikov, A.; Leszczynski, J.; Pettersson, L. G. M. *J. Phys. Chem. A* **2001**, *105*, 9528.
(25) Dove, P. M.; Han, N.; Yoreo, J. J. D. *Proc. Natl. Acad. Sci. U.S.A.* **2005**, *102*, 15357.
(26) Criscenti, L. J.; Kubicki, J. D.; Brantley, S. L. *J. Phys. Chem. A* **2006**, *110*, 198.
(27) Du, Z. M.; de Leeuw, N. H. *Dalton Trans.* **2006**, 2623.
(28) Yang, J.; Wang, E. G. *Phys. Rev. B* **2006**, *73*, 035406.
(29) Bickmore, B. R.; Wheeler, J. C.; Bates, B.; Nagy, K. L.; Eggett, D. L. *Geochim. Cosmochim. Acta* **2008**, *72*, 4521.
(30) Dove, P. M.; Han, N.; Wallace, A. F.; De Yoreo, J. J. *Proc. Natl. Acad. Sci. U.S.A.* **2008**, *105*, 9903.
(31) Nangia, S.; Garrison, B. J. *J. Phys. Chem. A* **2008**, *112*, 2027.
(32) Nangia, S.; Garrison, B. J. *Mol. Phys.* **2009**, *107*, 831.
(33) Luttge, A.; Bolton, E. W.; Lasaga, A. C. *Am. J. Sci.* **1999**, *299*, 652.
(34) Kawasaki, M.; Onuma, K.; Sunagawa, I. *J. Cryst. Growth* **2003**, *258*, 188.
(35) Arvidson, R. S.; Beig, M. S.; Luttge, A. *Am. Mineral.* **2004**, *89*, 51.
(36) Vinson, M. D.; Luttge, A. *Am. J. Sci.* **2005**, *305*, 119.
(37) Stefanovich, E. V.; Truong, T. N. *J. Chem. Phys.* **1997**, *106*, 7700.
(38) Shoemaker, J. R.; Burggraf, L. W.; Gordon, M. S. *J. Phys. Chem. A* **1999**, *103*, 3245.

10.1021/ja901305y CCC: $40.75

These advances are promising but have not yet uncovered all the complexities of the mineral−water interfaces. This is especially true for the quartz−water interface, where experimental studies show that quartz dissolution is a kinetically slow process,[1,19,31] and computational simulation of the process requires efficient rare-event sampling. These limitations have not allowed a clear picture of quartz−water dissolution to emerge, and there are several mechanistic aspects that still need to be explored.[25,30]

The key to understanding dissolution of quartz lies with its complex structure, which has only 0.2% impurity.[39] Although quartz is nearly pure, the geometrical structure has a rich tapestry that makes understanding the dissolution tricky. Before discussing prior studies, the nature of the surface structure and the associated nomenclature must be defined. Composed of Si and O atoms, quartz has an open, three-dimensional framework structure formed by corner-sharing SiO_4^{4-} tetrahedral units. At the surface, however, the Si−O bonds are capped by H atoms, forming hydroxyl groups. The surface Si centers vary in their connectivity to the bulk; therefore, we will follow the standard naming convention used in the literature.[40−43] Each Si atom is assigned a Q^i, label where i is the number of bridging bonds connecting the Si to the neighboring Si sites, and the remaining $(4 - i)$ surrounding groups are hydroxyls. A Q^2 Si, for example, has two hydroxyl groups and two bridging bonds to the neighboring Si sites, whereas a Q^4 Si has no hydroxyl groups and is embedded within the bulk. In contrast, a Q^0 Si has no bonds to the bulk and represents a free silicic acid molecule, $Si(OH)_4$. The Q^i labels are useful in systematically illustrating the dissolution process because the hydrolysis of each Si−O−Si bond can be represented simply as $Q^i \rightarrow Q^{i-1}$. This convention will be used throughout this article to present the structural changes that occur in the surface weathering process. Four relevant prior studies provide the background for the study presented here. The first study is an experimental one; the second study is electronic structure based; the third and fourth are probabilistic models.

Recently, Dove et al. studied the dissolution of amorphous silica and showed that, despite the lack of long-range order in amorphous silica, it shows similarities in the dissolution trends with crystalline forms.[30] The model used in their study highlighted the role of Q^2 and Q^3 sites as the two predominant reacting units that undergo dissolution to form Q^0 species in solution. Dove et al. proposed that the dissolution rate is governed by the removal of Q^2 sites because the reduced accessibility of the Q^3 sites inhibits their ability to react. They do not propose, however, any importance to the Q^1 site, the geometrically most accessible site. Although they give the importance of removal from a Q^2 site, they do not address the microscopic mechanism of how the quartz dissolves. In particular, does the Q^2 Si go directly into silicic acid in solution, or is there a stepwise process in which the Q^2 is converted to a Q^1 on the surface and then the dissolution occurs from a Q^1 site?

Part of the microscopic picture is obtained through several ab initio studies that have elucidated dissolution mechanisms for small silica clusters.[8,17,18,23,24,26,31] The calculations have identified the elementary steps involved in the hydrolysis of Si−O−Si bonds, the activation barriers, and the rate of dissolution over a wide 2−12 pH scale.[31] Within the ability of the ab initio techniques and the tractable system sizes, it is found that the energetics associated with dissolution from all Q^i sites are similar.[32] Going beyond the atomistic insight obtained from the small-cluster calculations, there is a need to incorporate the topological aspects and surface roughness to make a better judgment of the chemistry at the quartz−water interface.

In another set of computational studies, mineral surface roughness and its evolution have been simulated using kinetic models for systems that are far from equilibrium.[44−49] In these cases, the emphasis is usually to simulate flow experiments where dissolution products are continuously removed from the system, thus removing any possibility of precipitation. Theoretically, for an open flow-through system, the dissolution rate is kinetically controlled and depends on the activation energies of the various surface reactions.

In contrast, a batch-reactor experiment has both forward and backward reactions that eventually reach equilibrium. The reactions are therefore thermodynamically controlled and need simulation techniques very different from those used in the kinetically controlled flow-through systems. Simulating a thermodynamically controlled system was the focus of a recent study by Bandstra and Brantley, who used a stochastic model on a simplified two-dimensional (2D) system representing the mineral surface.[50] Their model incorporated four key concepts important to describe dissolution: (1) crystal structure, (2) probabilistic nature of reactive sites based on connectivity, (3) reversibility of the forward dissolution and the precipitation processes, and (4) crystal defects. Based on these features, the 2D system showed that mineral surfaces reach a steady-state conformation with time. This very interesting result shows that, despite an overly simplified 2D representation of the real mineral surface, the stochastic model was able to capture the evolution of the mineral surface. The probabilistic approach by Bandstra and Brantley shows promise; however, the structural details and full dimensionality of the system need to be incorporated.

In the present article, a new theoretical probabilistic approach is presented that uses advanced Monte Carlo (MC) techniques. Using this new approach, simulations are performed on a full three-dimensional quartz−water system complete with the details of the Q^i sites and explicit water molecules. The reversible reactions conditions will be considered with possibilities of dissolution, precipitation, and polymerization steps. The aim in this work is to focus on the qualitative aspects of the evolution of the quartz−water interface under thermodynamically controlled conditions.

The present article is organized in the following sections. Section II provides the theoretical basis of the work, and the computational details are presented in section III. The results

(39) Deer, W. A.; Howie, R. A.; Zussmann, J. *Rock-Forming Minerals*; Longmans: London, 1963; Vol. 4.
(40) Engelhardt, G.; Jancke, H.; Hoebbel, D.; Weiker, W. *Z. Chem.* **1974**, *14*, 109.
(41) Engelhardt, G.; Zeigan, D.; Jancke, H.; Hoebbel, D.; Weiker, W. *Z. Anorg. Allg. Chem.* **1975**, *418*, 17.
(42) Harris, R. K.; Newman, R. H. *J. Chem. Soc., Faraday Trans. 2* **1977**, *73*, 1204.
(43) Harris, R. K.; Knight, C. T. G. *J. Mol. Struct.* **1982**, *78*, 273.
(44) van Veenendaal, E.; van Beurden, P.; van Enckevort, W. J. P.; Vlieg, E.; van Suchtelen, J.; Elwenspoek, M. *J. Appl. Phys.* **2000**, *88*, 4595.
(45) Agger, J. R.; Hanif, N.; Anderson, M. W. *Angew. Chem., Int. Ed.* **2001**, *40*, 4065.
(46) Lasaga, A. C.; Luttge, A. *Am. Mineral.* **2004**, *89*, 527.
(47) Lasaga, A. C.; Luttge, A. *J. Phys. Chem. B* **2005**, *109*, 1635.
(48) Meakin, P.; Rosso, K. M. *J. Chem. Phys.* **2008**, 129.
(49) Zhang, L.; Luttge, A. *J. Phys. Chem. B* **2008**, *112*, 1736.
(50) Bandstra, J. Z.; Brantley, S. L. *Geochim. Cosmochim. Acta* **2008**, *72*, 2587.

and discussion are presented in sections IV and V, respectively. Finally, the conclusions are provided in section VI.

II. Theory

The objective of this study is to model the dissolution of quartz using a description that includes the full structure and chemistry of the solid and the solution phase. The method of choice is based on MC simulations in which configurations of Si groups on the surface and in solution are sampled to determine the equilibrium distribution. MC techniques allow for the explicit use of an interaction potential to describe the structure and energetics of the quartz−water system. The simplest form of MC moves involves, for example, randomly picking one molecule and placing it elsewhere in the system, attempting to find a lower energy configuration. The challenge here is that the reactive moves do not involve single atoms but rather clusters that have dissimilar sizes. For incorporating the reactions, we employ the reactive MC (RxMC) approach.[51,52] To allow for the interchange of the bulky surface group with several water molecules, we use the configurational bias MC (CBMC) technique.[53] Below we describe the MC methodology, the interaction potential used, and the algorithms developed specifically for quartz dissolution.

A. Combined Reactive and Configurational Bias Monte Carlo. The combined RxMC and CBMC techniques provide the required theoretical framework for studying the present silicate−water system. The RxMC scheme was developed independently by Smith and Triska[51] and Johnson et al.[52] Both groups were motivated to develop a MC protocol for systems where components underwent association dimerization and even hydrogen bonding. Since these early formulations, there have been several applications of RxMC methods.[54−59] A few years prior to the development of RxMC, the now popular CBMC method[53] was developed by Siepmann and Frenkel to make the MC simulations more efficient.[60−66] More recently, Jakobtorweihen et al. combined these two MC methods to study propene metathesis reaction in confined environments.[67] The present application also combines the RxMC and CBMC approaches with adaptations specific for mineral−water interfaces.

The advantage of the RxMC approach is that it provides a theoretical framework to study chemical properties of both forward and backward reactions, essential for the quartz−water surface chemistry. To describe the reaction where the bonds are broken and formed, it is impossible to preserve the identity of the molecules in the system with a fixed number of individual molecular components. This dilemma, however, is not a problem in RxMC because, unlike conventional MC, RxMC conserves the number of atoms in a system and not the identity of the individual molecules. The RxMC method is a well-developed technique, and for brevity only some key aspects are presented here.

The chemical reaction events are modeled by random deletion of the reactant molecules and insertion of the product molecules according to the stoichiometry of the reaction. The reactive chemical system can be completely defined in terms of the identity of the various chemical species and the stoichiometry of the overall chemical reaction:

$$\sum_{j=1}^{N_c} \nu_j M_j = 0 \tag{1}$$

where N_c is the number of unique chemical species in the system, ν_j is the stoichiometry of the jth chemical species, and M_j is the chemical symbol. In the above equation, the standard convention of associating positive and negative values to ν_j for reactants and products has been used. The sum over all components in the above equation is zero and represents the mass balance of the overall chemical process. The aim of this method is to find the transition probability P(new←old) due to the reactive process. The probability of finding the system in a given state is defined in terms of the Ξ grand canonical partition function:[52]

$$P_{old} = \frac{1}{\Xi} e^{-\beta U_{old}} e^{\beta \sum_{j=1}^{N_c} N_j \mu_j} \prod_{j=1}^{N_c} \frac{q_j^{N_j}}{N_j!} \tag{2}$$

where N_j, μ_j, and q_j are the number, chemical potential, and partition function of the jth component, respectively. The total potential energy is given by U_{old}, and $\beta = 1/k_B T$, where T is temperature and k_B is the Boltzmann constant. As the reaction proceeds, the system is transferred to a new state, and the number of the components changes from N_j to $(N_j + \nu_j)$. The probability of finding the system in the new configuration is defined as[52]

$$P_{new} = \frac{1}{\Xi} e^{-\beta U_{new}} e^{\beta \sum_{j=1}^{N_c} (N_j+\nu_j)\mu_j} \prod_{j=1}^{N_c} \frac{q_j^{N_j+\nu_j}}{(N_j+\nu_j)!} \tag{3}$$

The explicit expression for the transition probability P(new ← old) can be obtained using the following definition,

$$P(\text{new} \leftarrow \text{old}) = \frac{P_{new}}{P_{old}} \tag{4}$$

Substituting eqs 2 and 3 in the above expression,[52]

$$P(\text{new} \leftarrow \text{old}) = e^{-\beta(U_{new}-U_{old})} e^{\beta \sum_{j=1}^{N_c} \nu_j \mu_j} \prod_{j=1}^{N_c} \frac{N_j!}{(N_j+\nu_j)!} \prod_{j=1}^{N_c} q_j^{\nu_j} \tag{5}$$

By definition, any system in chemical equilibrium satisfies the following equation:

(51) Smith, W. R.; Triska, B. *J. Chem. Phys.* **1994**, *100*, 3019.
(52) Johnson, K.; Panagiotopoulos, A. Z.; Gubbins, K. E. *Mol. Phys.* **1994**, *81*, 717.
(53) Siepmann, J. I.; Frenkel, D. *Mol. Phys.* **1992**, *75*, 59.
(54) Pizio, O.; Henderson, D.; Sokolowski, S. *J. Phys. Chem.* **1995**, *99*, 2408.
(55) Segura, C. J.; Chapman, W. G. *Mol. Phys.* **1995**, *86*, 415.
(56) Muller, E. A.; Rull, L. F.; Vega, L. F.; Gubbins, K. E. *J. Phys. Chem.* **1996**, *100*, 1189.
(57) Turner, C. H.; Johnson, J. K.; Gubbins, K. E. *J. Chem. Phys.* **2001**, *114*, 1851.
(58) Turner, C. H.; Pikunic, J.; Gubbins, K. E. *Mol. Phys.* **2001**, *99*, 1991.
(59) Puibasset, J.; Pellenq, R. J. M. *J. Phys. Chem. B* **2008**, *112*, 6390.
(60) Frenkel, D.; Mooij, G.; Smit, B. *J. Phys.: Condens. Matter* **1992**, *4*, 3053.
(61) Siepmann, J. I.; Karaborni, S.; Smit, B. *Nature* **1993**, *365*, 330.
(62) Siepmann, J. I.; McDonald, I. R. *Phys. Rev. Lett.* **1993**, *70*, 453.
(63) Smit, B.; Karaborni, S.; Siepmann, J. I. *J. Chem. Phys.* **1995**, *102*, 2126.
(64) Martin, M. G.; Siepmann, J. I. *J. Phys. Chem. B* **1998**, *102*, 2569.
(65) Vlugt, T. J. H.; Martin, M. G.; Smit, B.; Siepmann, J. I.; Krishna, R. *Mol. Phys.* **1998**, *94*, 727.
(66) Wick, C. D.; Martin, M. G.; Siepmann, J. I. *J. Phys. Chem. B* **2000**, *104*, 8008.
(67) Hansen, N.; Jakobtorweihen, S.; Keil, F. J. *J. Chem. Phys.* **2005**, *122*, 11.

$$\sum_{j=1}^{N_c} \nu_j \mu_j = 0 \tag{6}$$

Substituting the equilibrium condition, the final expression for the transition probability is[52]

$$P(\text{new} \leftarrow \text{old}) = \mathrm{e}^{-\beta(U_{\text{new}}-U_{\text{old}})} \prod_{j=1}^{N_c} \frac{N_j!}{(N_j+\nu_j)!} \prod_{j=1}^{N_c} q_j^{\nu_j} \tag{7}$$

The above derivation provides a generic expression for calculating the transition probability of any reactive system, but there is a caveat in applying this to reactive systems in dense media. If the simulation requires generating new configurations by insertion of a physically large molecule into a dense medium, then the transition probability for such a move system will be very small, and almost all reactive moves will be rejected. It is therefore necessary to combine the reactive moves with an efficient technique that overcomes this problem.

The CBMC technique is a practical solution to carry out simulations of systems that involve components with very dissimilar densities and molecular structures. In reactive systems, the reactants and products can have very different structures and exist in different phases. The reactive event requires insertion of product into another phase at a random coordinate that might overlap with other molecules and have a low-acceptance probability. The frequent occurrences of such low-acceptance events plague the MC calculations, making them computationally expensive. A CBMC method is a suitable solution for this problem, and in the original CBMC paper,[53] a polymer chain was allowed to grow bead by bead in a set of trial moves biasing the simulation away from low-acceptance events. The approach adopted in the present work is similar in spirit to the original CBMC method, but instead of growing the product molecule of a reaction event, the simulation is carried out through cluster moves.

More specifically, in the silicate−water system, the forward dissolution event leads to consumption of one water molecule per formation of an aqueous silicic acid in bulk water, and the back precipitation reaction leads to the formation of water and the bridging of the free silicic acid back onto the mineral surface or polymerization in solution. The components that are exchanged in forward and backward reactions are silicic acid and water, which have a 1:4 volume ratio (density of water at 1 g/cm^3). The configuration bias scheme is invoked by first deleting a randomly selected water molecule from bulk water and then substituting a silicic acid molecule in its place. The newly inserted silicic acid, with about 4 times the volume of a water molecule, overlaps with the surrounding water molecules. These overlapping water molecules are removed and then reinserted randomly back into bulk water using the Rosenbluth weighting factor.[68] The Rosenbluth weighting factor has been used extensively[69−74] for the configuration bias scheme and is described in more detail elsewhere.[53,67]

B. Potential Energy Function. The Fueston−Garofalini (FG) potential energy function V_{FG} has been used in the present work, as it has a successful track record of simulating silicate−water interaction in previous studies.[75] The FG potential energy function is a sum of modified two-body and three-body terms from earlier work, along with a modified Rahman−Stillinger−Lemberg potential.[76,77] The FG potential for a system with N particles is represented as

$$V_{FG} = \sum_{i\neq j}^{N} V_{ij} + \sum_{i\neq j\neq k}^{N} V_{jik} \tag{8}$$

where V_{ij} and V_{jik} are the two-body and three-body interaction terms, respectively. The interaction between atoms i and j is

$$V_{ij} = A_{ij}\,\mathrm{e}^{(-r_{ij}/\rho_{ij})} + \frac{q_i q_j}{4\pi\varepsilon_0 r_{ij}} \operatorname{erfc}\left(\frac{r_{ij}}{\beta_{ij}}\right) + \frac{a_{ij}}{1+\mathrm{e}^{(b_{ij}(r_{ij}-c_{ij}))}} \tag{9}$$

where r_{ij} is the internuclear distance between atoms i and j, q_i is the formal charge on atom i, ϵ_0 is the permittivity of free space, and A_{ij}, β_{ij}, ρ_{ij}, a_{ij}, b_{ij}, and c_{ij} are adjustable parameters. The V_{jik} term is

$$V_{jik} = \lambda_{ijk}[\cos(\theta_{jik}) - \cos(\theta^0_{jik})]^2 \exp\left(\frac{\gamma_{ij}}{r_{ij}-r^0_{ij}} + \frac{\gamma_{ik}}{r_{ik}-r^0_{ik}}\right) \quad \text{for} \quad r_{ij} < r^0_{ij} \quad \text{and} \quad r_{ik} < r^0_{ik}$$

$$= 0 \qquad \text{otherwise} \tag{10}$$

where θ_{jik} is the angle subtended by r_{ij} and r_{ik}, i being the vertex atom, and λ_{jik}, γ_{ij}, γ_{ik}, θ^0_{jik}, r^0_{ij}, and r^0_{ik} are adjustable parameters. For a given atom, a cutoff distance of 5.5 Å was used to calculate all forces. All the adjustable parameters have been reported in the literature previously and are not repeated here.[78]

C. Methodology and Algorithms. Reactive MC requires a suite of reaction steps from which to choose in any particular simulation move. The simulations were carried out using the direct and stepwise approaches. The motivation is to test the two approaches since the actual dissolution mechanism is not fully understood. The comparison of the two approaches will possibly contrast their differences and help test the present methodology.

The direct approach always leads to dissolution by hydrolyzing the surface bonds and leading to the formation of a Q^0 species in bulk water. The overall process involves picking a reactive Si site at random, hydrolyzing all the O_{br} bridged bonds, and deleting one water molecule from the bulk water per Si−O_{br}−Si bond hydrolyzed. The selection of water molecules to be deleted is random. The back reaction of the Q^0 species onto the silicate surface or polymerization in solution is considered with a Boltzmann probability. The direct approach algorithm is straightforward to implement, and the detailed steps are depicted as a flowchart in Figure 1. The forward reaction of a Q^1 site hydrolysis with a Q^i neighbor is represented as

(68) Rosenbluth, M. N.; Rosenbluth, A. W. *J. Chem. Phys.* **1955**, *23*, 356.
(69) Sariban, A.; Binder, K. *Macromolecules* **1988**, *21*, 711.
(70) Lyubartsev, A. P.; Martsinovski, A. A.; Shevkunov, S. V.; Vorontsovvelyaminov, P. N. *J. Chem. Phys.* **1992**, *96*, 1776.
(71) Panagiotopoulos, A. Z. *Mol. Simul.* **1992**, *9*, 1.
(72) Hao, M. H.; Scheraga, H. A. *J. Phys. Chem.* **1994**, *98*, 4940.
(73) Vasquez, M.; Nemethy, G.; Scheraga, H. A. *Chem. Rev.* **1994**, *94*, 2183.
(74) Dellago, C.; Bolhuis, P. G.; Csajka, F. S.; Chandler, D. *J. Chem. Phys.* **1998**, *108*, 1964.
(75) Feuston, B. P.; Garofalini, S. H. *J. Phys. Chem.* **1990**, *94*, 5351.
(76) Stillinger, F. H.; Rahman, A. *J. Chem. Phys.* **1978**, *68*, 66.
(77) Stillinger, F. H.; Weber, T. A. *Phys. Rev. B* **1985**, *31*, 5262.
(78) Litton, D. A.; Garofalini, S. H. *J. Appl. Phys.* **2001**, *89*, 6013.

$$Q^i{-}O_{br}{-}Q^1(s) + H_2O \rightarrow Q^{i-1} + Q^0(aq) \quad (11)$$

Similarly, the Q^2 and Q^3 sites also undergo hydrolysis using two and three water molecules in the process

$$[Q^i{-}O_{br}]_2{-}Q^2(s) + 2H_2O \rightarrow 2Q^{i-1} + Q^0(aq) \quad (12)$$

$$[Q^i{-}O_{br}]_3{-}Q^3(s) + 3H_2O \rightarrow 3Q^{i-1} + Q^0(aq) \quad (13)$$

and reducing the coordination of all their neighbors to Q^{i-1}. The back reaction in this case will be just the reverse of eq 11, with free Q^0 species precipitating on the surface or polymerizing in solution.

In contrast to the direct approach, in the stepwise approach only one $Si{-}O_{br}{-}Si$ bond is hydrolyzed in each MC step. The protocol for the hydrolysis of the bond is intricate and requires knowledge of the Q^i numbers of the selected Si site and its neighboring Si sites. In the case of Q^2 and Q^3 sites with more than one $Si{-}O_{br}{-}Si$ bridged bonds, it is more efficient to hydrolyze the bond with the least coordinated neighbor. In Table 1, an extended list of reactive sites and neighbors is provided, along with the specific bond that is hydrolyzed using the least coordinated protocol. The aim of developing this protocol is to simulate a more chemically realistic method. For example, if a selected site is Q^2, with Q^2 and Q^4 as its two neighbors, then it is more likely that the Q^4 bulk site farther from the surface is less accessible for dissolution, while the less coordinated Q^2 site is more readily hydrolyzed by water. Also, by using the least coordinated protocol, the simulation algorithmically is more efficient, as fewer sterically hindered moves with low-acceptance probability events are generated. Another consequence of the least coordinated protocol is that, for cases where a selected Q^2 or Q^3 site has a Q^1 neighbor, the bond to Q^1 is hydrolyzed, which is similar to shifting the reaction center to the Q^1 site. In case of the back reaction, the algorithmic protocol is very general and picks precipitation sites scholastically, allowing both surface precipitation and polymerization in solution. The flowchart in Figure 2 shows the implementation of the least coordinated protocol step by step.

III. Computational Details

The simulations were carried out using a locally developed modular MC program written in FORTRAN 90. The FG potential was also programmed using the functional form and corrected parameters from the literature.[78] The structure of α-quartz is hexagonal with space group $P3_121$ and a unit cell of $a = b = 4.914$ Å, $c = 5.405$ Å, $\alpha = \beta = 90°$, and $\gamma = 120°$. For the simulations, two α-quartz and water systems were designed that have different ratios of Q^i sites. System I is a smaller test system with a 7 Å radius α-quartz crystallite in the center of a cubic water box of dimensions 22 Å × 22 Å × 22 Å with 1 g/cm^3 density. System II has a 12 Å radius α-quartz crystallite enclosed in a 30 Å × 30 Å × 30 Å box of water as shown in Figure 3. The simulations were performed for both systems I and II, and both showed similar trends in the results. Therefore, for clarity in the discussion, all the results reported in the following sections are for the larger system II at 500 K unless specifically mentioned otherwise. In the temperature effect studies, the simulation included lower temperatures in the 300−500 K range.

IV. Results

A. Direct Mechanism. The direct mechanism results in dissolution of a surface site at each successful MC step. There are, however, three types of surface sites, and these can be tested systematically by modeling systems with restricted combinations of Q^i sites that hydrolyze and precipitate. The simplest simulation is the Q^1-dissolution, in which only the Q^1 sites are sampled for the dissolution and precipitation reactions. The next hierarchical simulation is the Q^1Q^2-direct dissolution, where both Q^1 and the Q^2 sites are allowed to undergo reactions. Finally,

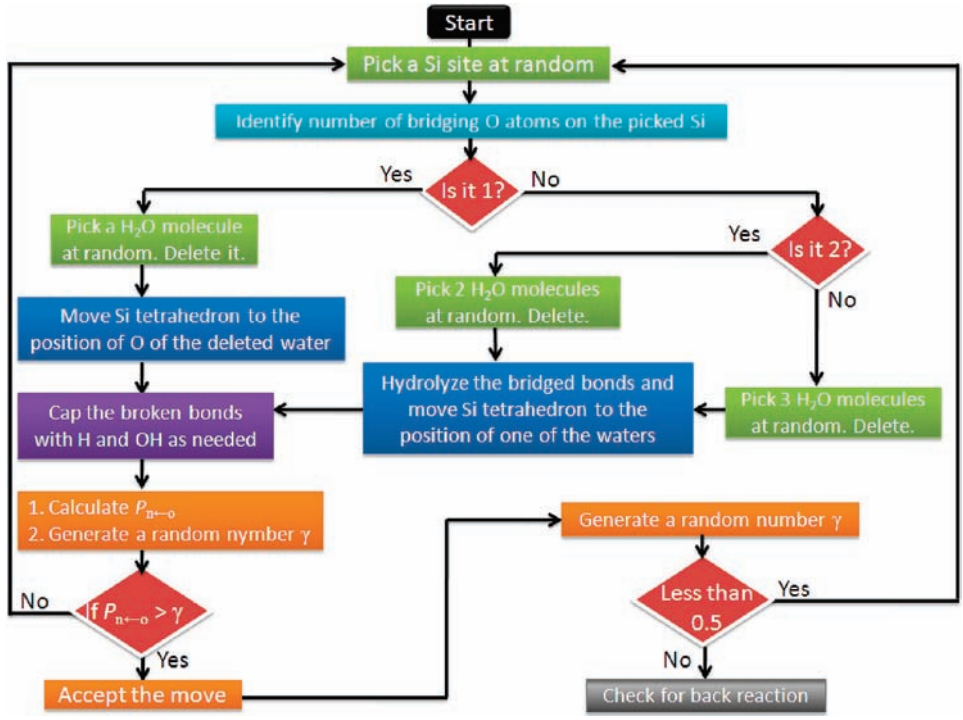

Figure 1. Flowchart for the steps involved in the direct dissolution algorithm.

Table 1. Least Coordinated Protocol Used in the Stepwise Approach

reaction center	bonded neighbors: first	second	third	selected neighbor
Q^1	Q^2			Q^2
	Q^3			Q^3
	Q^4			Q^4
Q^2	Q^1	Q^2		Q^1, move reaction center
	Q^1	Q^3		Q^1, move reaction center
	Q^1	Q^4		Q^1, move reaction center
	Q^2	Q^3		Q^2
	Q^2	Q^4		Q^2
	Q^3	Q^4		Q^3
	Q^4	Q^4		Q^4
Q^3	Q^1	Q^1	Q^2	randomly select first or second Q^1, move reaction center
	Q^1	Q^1	Q^3	randomly select first or second Q^1, move reaction center
	Q^1	Q^1	Q^4	randomly select first or second Q^1, move reaction center
	Q^1	Q^2	Q^2	Q^1, move reaction center
	Q^1	Q^2	Q^3	Q^1, move reaction center
	Q^1	Q^2	Q^4	Q^1, move reaction center
	Q^1	Q^3	Q^3	Q^1, move reaction center
	Q^1	Q^3	Q^4	Q^1, move reaction center
	Q^1	Q^4	Q^4	Q^1, move reaction center
	Q^2	Q^2	Q^2	randomly select first, second, or third Q^2
	Q^2	Q^2	Q^3	randomly select first or second Q^2
	Q^2	Q^2	Q^4	randomly select first or second Q^2
	Q^2	Q^3	Q^3	Q^2
	Q^2	Q^3	Q^4	Q^2
	Q^2	Q^4	Q^4	Q^2
	Q^3	Q^3	Q^3	randomly select first, second, or third Q^3
	Q^3	Q^3	Q^4	randomly select first or second Q^3
	Q^3	Q^4	Q^4	Q^3
	Q^4	Q^4	Q^4	randomly select first, second, or third Q^4

the $Q^1Q^2Q^3$-direct dissolution, as the name suggests, involves sampling of Q^1, Q^2, and Q^3 sites.

The progress of system I at 500 K is monitored for all three sampling protocols. The fraction of Si atoms in the system as Q^0 (i.e., silicic acid molecules in solution) generated at each MC step is calculated, as shown in Figure 4. The results show two very different behaviors, one leading to steady state as in the Q^1-dissolution, and the other two leading to complete dissolution.

In the Q^1-dissolution simulation, initially the Q^1 sites hydrolyze to form the Q^0 species in solution. With the increase in the concentration of Q^0 species, precipitation reactions occur

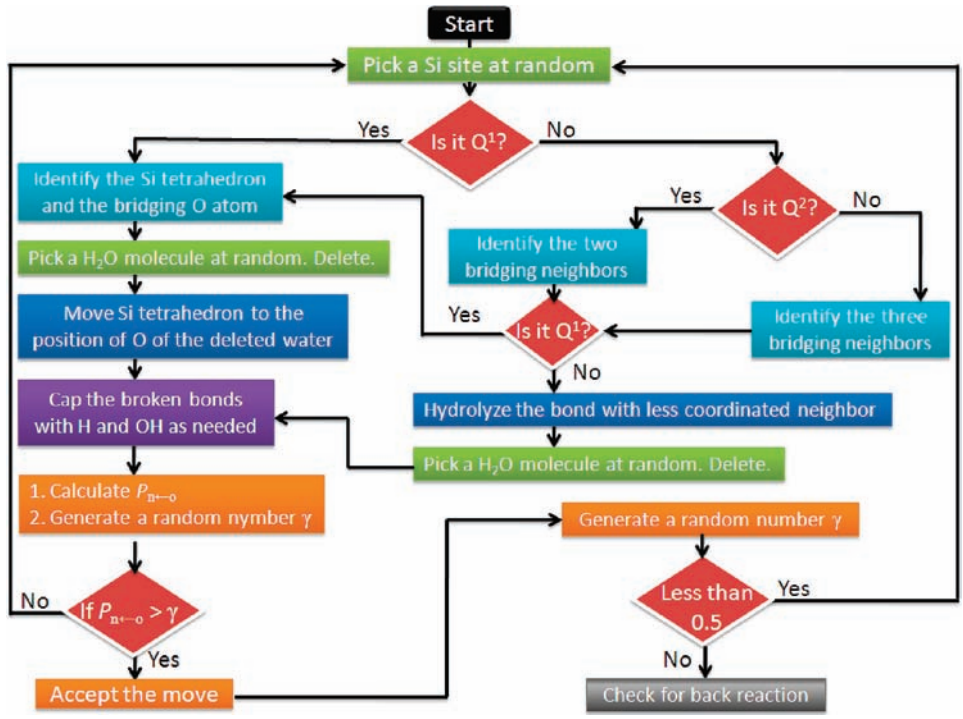

Figure 2. Flowchart for the steps involved in the stepwise dissolution algorithm.

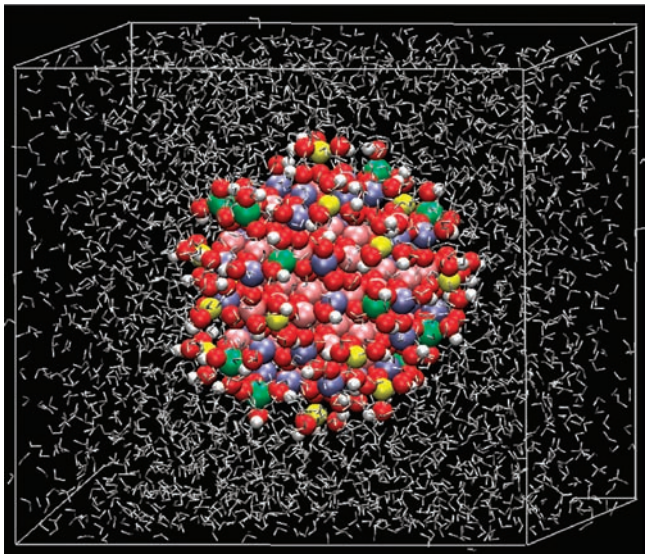

Figure 3. Snapshot of initial simulation setup of a 12 Å α-quartz crystallite enclosed in a 30 Å × 30 Å × 30 Å box of water. The Si sites are shown as Q^1 (yellow), Q^2 (green), Q^3 (blue), and Q^4 (pink). The silicate oxygen and hydrogen atoms are shown in red and white, respectively. To highlight the quartz crystallite, the water molecules are shown in gray.

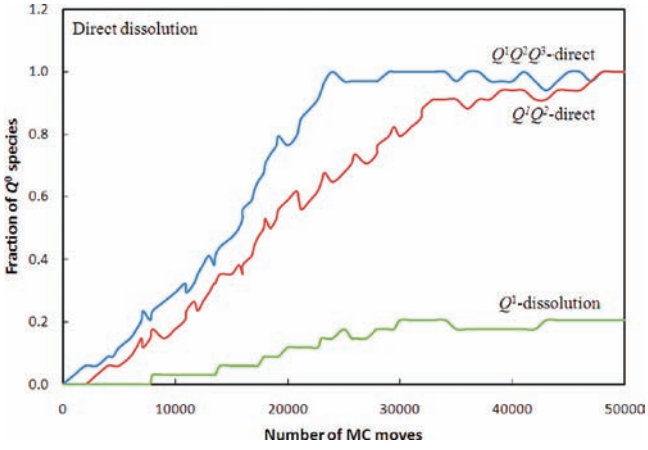

Figure 4. Plot of the fraction of Si in solution obtained using $Q^1Q^2Q^3$-direct, Q^1Q^2-direct, and Q^1-dissolution algorithms as a function of number of MC moves at 500 K.

(denoted by a decrease in the Q^0 fraction), eventually reaching a steady state. The forward and backward reactions lead to several Q^1 and Q^0 exchanges. A closer look at the evolution of the quartz crystallite surface in the Q^1-dissolution simulation shows that removal of Q^1 sites in the dissolution process occurs irrespective of the underlying surface site. This indifference to the Q^i number of the neighboring Si is in agreement with the previous ab initio calculations on silica clusters,[32] where it was found that the barrier heights of $Q^1-O_{br}-Q^i$ are almost similar for $i = 1-4$. The Q^1-dissolution simulation reaches a steady state with a Q^0 fraction of ~0.19. The surface of the crystallite at equilibrium consists of Q^2 and Q^3 sites with an occasional Q^1 site. Thus, if dissolution occurs only from Q^1 sites, there will never be complete dissolution of the sample.

In contrast, the Q^1Q^2-direct dissolution and $Q^1Q^2Q^3$-direct dissolution simulations lead to complete dissolution of the quartz crystallite with a Q^0 species fraction of ~1 toward the end of the simulation, as shown in Figure 4. Experimentally, it is observed that quartz dissolution is very difficult and is a very slow process.

Table 2. Average Distribution of the Q^i Sites for Three Mechanisms for Five Runs at 500 K

	Q^0	Q^1	Q^2	Q^3	Q^4
		System I			
Q^1-dissolution	0.19	0.04	0.12	0.37	0.28
Q^1Q^2-stepwise	0.17	0.04	0.11	0.39	0.29
$Q^1Q^2Q^3$-stepwise	0.19	0.05	0.13	0.35	0.28
		System II			
Q^1-dissolution	0.13	0.02	0.13	0.43	0.29
Q^1Q^2-stepwise	0.11	0.11	0.11	0.37	0.29
$Q^1Q^2Q^3$-stepwise	0.13	0.17	0.17	0.26	0.27

Thus, the dissolution through Q^1Q^2- and $Q^1Q^2Q^3$-direct dissolution mechanisms is not realistic. There are other factors that also argue against this mechanism. First, the direct dissolution involves breaking of two or three bridge bonds, each with a gas-phase barrier height[31] of 159 kJ/mol, versus only one bridge bond for the Q^1-dissolution. This energy cost is quite high. Second, there is limited accessibility of these sites for water molecules to carry out bond-breaking. Third, in general, for there to be several simultaneous bond breaks, there should be some linkage as to why they must occur together. At this point, we cannot justify any reason. Although the Q^1Q^2- and $Q^1Q^2Q^3$-direct dissolution approaches are potentially not the real mechanisms for dissolution of silicates, they nevertheless are good test cases for developing the MC methodology and contrasting the behavior of the Q^1-dissolution approach.

B. Stepwise Mechanism. The stepwise mechanism is tested in a hierarchical way developed in the previous section; however, the naming convention for the simulations is now Q^1-dissolution (same as direct mechanism), Q^1Q^2-stepwise, and $Q^1Q^2Q^3$-stepwise. Simulations were performed using all three mechanisms for systems I and II, and the results averaged over five runs are presented in Table 2.

The simulation on system I shows that the fraction of the Q^0 sites is almost independent of the stepwise mechanism employed to obtain the results. Since the stepwise and direct algorithms are the same for Q^1-dissolution, the same 0.19 site fraction is obtained. The other results for the simulations show similar trends for both systems I and II. For the remainder of this section, we will analyze the results for system II to illustrate the dissolution steps and the evolution of Q^i sites; each of the mechanisms is discussed in detail.

The plots of the fraction of the total system for each Q^i species as a function of number of MC moves are shown in Figures 5−7. For Q^1-dissolution as shown in Figure 5, the first trend is the gradual growth of the Q^0 species in solution until about 60 000 MC steps, where it plateaus until about 155 000 steps, followed by a single dissolution move that eventually precipitates after the next 10 000 moves. As expected, the increase of Q^0 is inversely related to the dissolution trend of Q^1 species and reduces to very small percentage of the total surface fraction by 200 000 MC steps. The trends also show that the Q^1 dissolution occurs from Q^4 sites, indicated by a gradual decrease of Q^4 and the reverse buildup of the Q^3 species. There have also been a few steps where Q^1 has hydrolyzed off a Q^3 site, resulting in an increase of Q^2 sites that, after about the initial 5000 steps, remains unchanged throughout the rest of the simulation. The overall ratios of Q^i species in the end of the simulation are shown in Table 2 and will be compared with other data later in this section.

The surface species fractions from the Q^1Q^2-stepwise simulation are plotted in Figure 6. Compared to the Q^1-dissolution

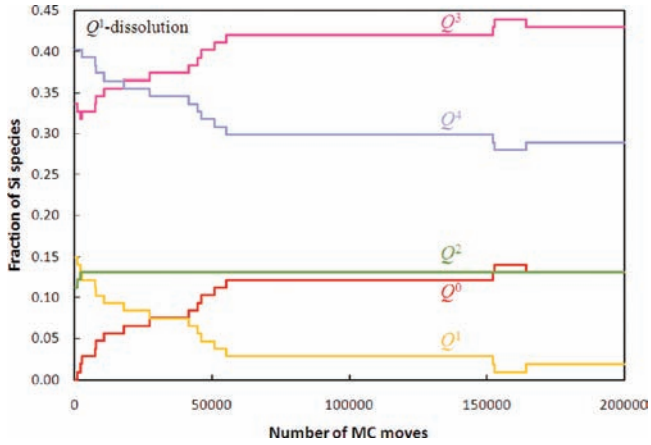

Figure 5. Evolution of Q^i species fraction simulated using the Q^1-dissolution algorithm as a function of number of MC moves at 500 K.

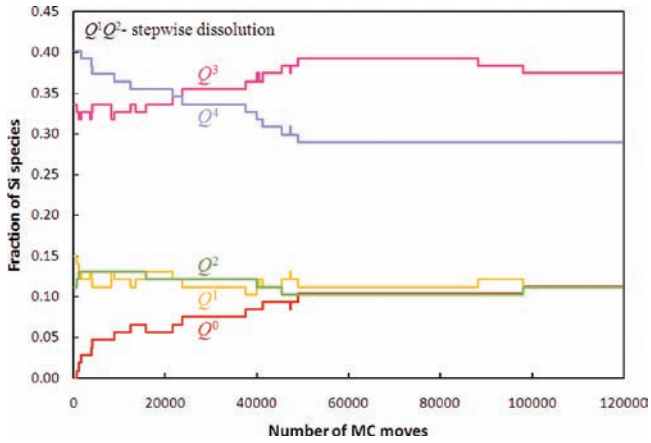

Figure 6. Evolution of Q^i species fraction simulated using the Q^1Q^2-stepwise dissolution algorithm as a function of number of MC moves at 500 K.

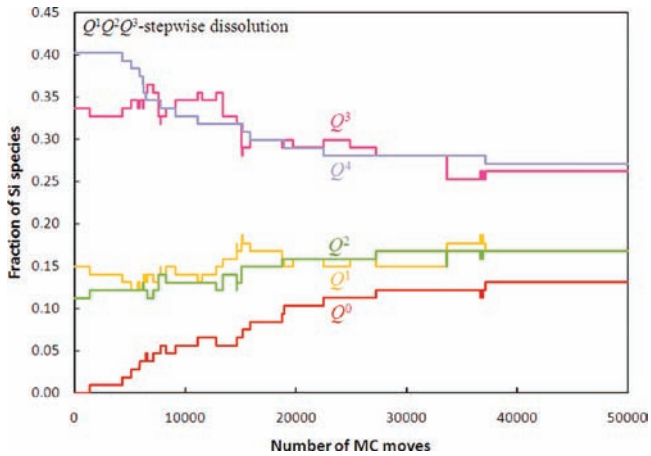

Figure 7. Evolution of Q^i species fraction simulated using the $Q^1Q^2Q^3$-stepwise dissolution algorithm as a function of number of MC moves at 500 K.

simulation, the Q^1Q^2-stepwise simulation reaches a steady state in a fewer number of MC steps (~120 000). The Q^0 fraction shows an initial increase, but unlike in the Q^1-dissolution case, the species trend is influenced by the role of Q^2 species. The Q^2 fraction shows small fluctuations in the simulations, though the surface fraction before and after the simulation remains almost unchanged at about 0.11. The Q^2 hydrolysis is sterically difficult and results in formation of at least one Q^1 species and another Q^{i-1}species, depending on the neighboring Q^i site, as shown in Table 1. An important aspect of this mechanism is highlighted by the increase in the fluctuations of the all the Q^i species compared to the trends in Figure 5. The average steady-state Q^i fractions' data are presented in Table 2 for comparison with Q^1-dissolution results.

The Q^i species fractions as a function of MC steps for the $Q^1Q^2Q^3$-stepwise surface evolution are presented in Figure 7. The fluctuation of surface speciation and complexity of reactions increases tremendously compared to the Q^1-dissolution and Q^1Q^2-stepwise simulations shown in Figures 5 and 6. The Q^1 species gradually increase in the solution, showing several forward and backward reactions that can be mapped to complex steps shown in Table 1. The same is true for the other Q^i sites, except the Q^4 fraction, which shows only a decrease as the simulation progresses. The steady-state surface conformation is achieved in a smaller number (~50 000) of simulation steps than in previous simulations. The reason for this observation is mainly algorithmic, as all the sites (Q^1, Q^2, and Q^3) on the surface are being sampled in the $Q^1Q^2Q^3$-stepwise mechanism. Any accepted dissolution move of a Q^2 or Q^3 site opens twice as many sites for further participation in precipitation or dissolution events, leading to the steady state in a fewer number of steps. This trend has been observed for five separate simulations, and the average Q^i fraction for $Q^1Q^2Q^3$-stepwise mechanisms is reported in Table 2.

A very clear trend emerges from the comparison of the Q^i data in Table 2. Namely, the Q^1-dissolution, Q^1Q^2-stepwise, and $Q^1Q^2Q^3$-stepwise mechanisms all yield almost the same Q^0 fraction in solution. Similarly, the Q^4 bulk species fraction attains a nearly constant value of 0.29, averaged over five simulation runs and the three mechanisms. The only differences in the three mechanisms are in fractions of the Q^1, Q^2, and Q^3 surface species. This can be explained by the disparity in the hydrolysis protocols for mechanisms, but on an average, none of these mechanisms lead to complete dissolution and all reach a steady-state dissolution state. Furthermore, this confirms that, even though the Q^2 and Q^3 hydrolysis events do occur, they are compensated by the backward precipitation reactions and do not contribute significantly toward the formation of Q^0 species. The important result of this study is that it is able to demonstrate, without the use of expensive time-progression simulations, that inclusion of Q^2 and Q^3 contributions to the Q^1-dissolution mechanisms does not alter the fraction of Q^0 species in solution.

C. Temperature Effects. The temperature effects were studied for 300, 400, and 500 K using the Q^1-dissolution mechanism, and the results for the evolution of Q^0 species as a function of MC steps are shown in Figure 8. The Q^1Q^2- and $Q^1Q^2Q^3$-stepwise mechanisms yielded results similar to those obtained with the Q^1-dissolution mechanism and are therefore not included here. The 300 and 400 K temperature simulations show fewer dissolution steps that lead to a steady state with no precipitation events; however, for the 500 K simulation, several dissolution steps occurred, followed by precipitation. The increase in the number of Q^0 species with increase in temperature is in agreement with the experimental observations.[1,19]

V. Discussion

In this section, a discussion of the highlights of the results is provided along with a comparison to previous experimental and theoretical models. The present study successfully goes beyond the previous small-cluster calculations to include a realistic

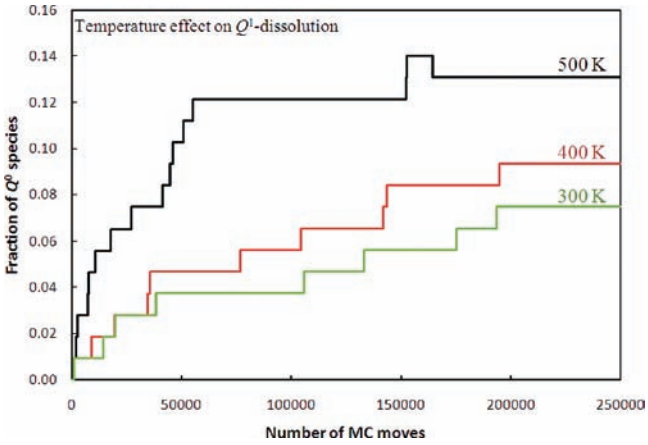

Figure 8. Effect of temperature on the evolution of Q^0 species in solution, simulated using the Q^1-dissolution algorithm at 300, 400, and 500 K.

description of a quartz crystallite in contact with explicit water molecules. The major observations of this study are that direct dissolution from Q^2 and Q^3 sites is less probable than dissolution from Q^1 sites, and for stepwise dissolution mechanisms, the fraction of Q^0 species (silicic acid molecules in solution) is independent of the Q^i surface sites that participate in the dissolution mechanism.

A key result here is that the amount of silicic acid in solution depends on the number of initial Q^1 sites. This result is unlike a typical solubility product, in which the amount of dissolved solid is constant for a unit volume of water (per liter). Thus, even though our calculations are for equilibrium conditions, they make an implication for the kinetics of dissolution. The simulations show that, once the Q^1 sites on the surface are depleted, the dissolution process is essentially terminated, indicating that overall dissolution will appear to be kinetically slow. It is chemically sensible that the predominant dissolution reaction occurs for a Q^1 site that has only one bond to the bulk mineral. The conclusions of Q^1 reactivity are based on the simulation of quartz crystallite and are not any specific to any low- or high-index Miller plane of quartz. The variation of due morphological factors was not the focus of this article, but such simulations will be performed in subsequent studies.

Although these calculations have been performed for quartz using an interaction potential designed for neutral reactions, we believe that the topological argument should carry over to other conditions. For example, there are many polymorphs of silica with tetrahedral arrangements of SiO_4^{4-} units. Similarly, the surface groups can be protonated and deprotonated depending on the pH. The extra or missing proton, however, will not alter the basic topology. We propose that the same conclusion as to the dominance of the Q^1 dissolution would apply for other polymorphs of silica as well as the protonated and deprotonated states. Any defects or impurities that increase the number of Q^1 sites will enhance dissolution, and any surface contaminants that bind to the Q^1 sites will inhibit dissolution. Furthermore, the analyses of the reactions on the quartz−water surfaces involving the intricate role of Q^i sites in both the dissolution and the precipitation steps, all leading to a formation of a steady state, conclusively show the inertness of silica for complete dissolution.

Comparing the results of the stepwise simulations to the experimental studies shows agreement regarding the lower accessibility of the Q^3 versus the Q^2 sites. There are, however, differences in the dissolution mechanism observed in the simulations and the model proposed by Dove et al.[30] Unlike the "plucking off" model of removal of Q^2 and Q^3 sites, our simulations show that the dissolution occurs through a stepwise mechanism with the key involvement of the reactive Q^1 sites. Additionally, Dove et al.[30] do not discuss how the precipitation reactions affect the overall dissolution, but the simulations show that back reaction of the Q^0 group (silicic acid) occurs on a surface site, creating Q^1 sites that cap the underlying surface sites from being hydrolyzed.

The simulation results are in good agreement with the observations of the Bandstra and Brantley simulation studies.[50] Using similar key concepts of dissolution processes but with an entirely different scheme, the present approach was able to go beyond the 2D model system, test possible dissolution mechanisms, and show the role of Q^i sites at the quartz−water interface in a real three-dimensional system surrounded with explicit water molecules. Both their study and the one presented here indicate the formation of steady-state conformation of the surface that is temperature dependent.

VI. Conclusions

The new MC approach provides a novel way to identify the reactions that are responsible for the weathering of the quartz surface. To accomplish these simulations, new protocols specifically designed for the quartz−water interface were implemented into existing advanced methods of reactive Monte Carlo and configuration bias Monte Carlo. In this study, the time progression was not followed, but rather the local arrangement of reactive sites on the quartz surface was explored in the presence of explicit water solvation. There are several conclusions that can be drawn from this study.

(i) The direct dissolution mechanism, similar to "plucking off" Q^2 and Q^3 sites from the surface to form Q^0 species in solution, leads to complete dissolution and is thus not realistic.

(ii) The dissolution and precipitation reactions occur via a stepwise mechanism predominantly from Q^1 sites, resulting in a steady-state surface conformation.

(iii) Dissolution of Q^1 sites occurs most often irrespective of the connectivity of the underlying Q^i site.

(iv) The Q^2 sites undergo hydrolysis to form a Q^1 and another Q^{i-1} site from a Q^i neighbor. This process is less common than the Q^1 site dissolution, as it leads to the formation of sterically crowded groups that reorient on the surface to adopt a stable structure but occupy the same general volume domain before the hydrolysis and are energetically less probable.

(v) The stepwise dissolution of Q^3 is energetically costly and is less frequent, and it is explained using the same arguments as for Q^2 dissolution.

(vi) The contributions of Q^2 and Q^3 hydrolysis events are compensated by precipitation reactions, and these do not significantly affect the fraction of Q^0 in solution.

(vii) Temperature effects show enhanced dissolution and precipitation events that eventually lead to a steady-state conformation specific to that temperature.

It is evident from the present work that quartz dissolution occurs via the hydrolysis of one Si−O−Si group at a time and is governed by the steric factors of the local connectivity of the surface Si sites. It shows the importance of surface topography in determining the reactivity and the chemistry of the surface.

Acknowledgment. This work has been supported by the National Science Foundation under the Grant No. CHE-0535656.

JA901305Y